Biophysical Journal, Volume *116*

Supplemental Information

CcdB at pH 4 Forms a Partially Unfolded State with a Dry Core

Chetana Baliga, Benjamin Selmke, Irina Worobiew, Peter Borbat, Siddhartha P. Sarma, Wolfgang E. Trommer, Raghavan Varadarajan, and Nilesh Aghera

Methods

REES measurements.

Red edge excitation shift measurements were done by exciting protein at 295, 300 and 305 nm using bandwidths of 1, 1 and 1.5 nm, respectively. Emission was collected from 320 to 380 nm using a bandwidth of 10 nm. Fluorescence emission spectra were collected using a data pitch of 1 nm and integration time of up to 15 seconds.

Thermal Stability Studies

Thermal stability was determined using fluorescence based thermal unfolding studies (1), carried out on an iCycle iQ5 Real Time Detection System (Bio-Rad, Hercules, California). A 20 µl reaction mixture having 4µM CcdB protein (at pH 7, in 10 mM HEPES or at pH 4, in 10 mM Sodium acetate) containing 2.5X Sypro orange dye, was subjected to thermal denaturation by varying the temperature from 40^{o}C to 95^{o}C with an increment of 0.5^{o}C/min. Denaturation of the protein was also carried out in the presence of 10µM CcdA peptide. Sypro orange binds to the exposed hydrophobic patches of a protein, leading to an increase in the detected fluorescence of the dye as the protein unfolds (1). The change in fluorescence signal with respect to temperature was analyzed. A relative fluorescence plot was generated by normalizing the values in the transition region, to the unfolded and folded baseline signals. The midpoint of the thermal unfolding curve (the temperature at which 50% of the protein is unfolded) was taken to represent the T_m.

Analytical ultracentrifugation

All sedimentation experiments were performed using a Beckman Optima XL-A ultracentrifuge. Sedimentation velocity data were analyzed with the UltraScanIII software program, version 3.3 (2). The sedimentation of CcdB at pH 4 and at pH 7 was monitored with

time, by measuring absorbance at 268nm and 281 nm, respectively. Wavelength scans were taken at the start of the experiment to determine the λ_{max} for absorbance for the sample. All measurements were at 20°C, and at 60,000 rpm, using standard Epon two-channel centerpieces. Samples used were CcdB at pH 7 (10 mM Hepes, 50 mM NaCl) and at pH 4 (10mM Sodium acetate, 50 mM NaCl), where the reference cell had the buffer alone. Hydrodynamic corrections for buffer density and viscosity were made according to methods outlined by Laue et al. (3) and as implemented in UltraScan. The data were analyzed by two-dimensional spectrum analysis (2D-SA) (4). Molecular weight and shape distributions obtained in the two-dimensional spectrum analysis were further refined by Monte Carlo (5) and GA analysis (6). This resulted in identification of the various species, with different sedimentation coefficients and frictional ratios that collectively gave rise to the sedimentation velocity profile. Boundary effects and differential radial dilution rates for the different components in the system were taken care of by the enhanced van Holde – Weischet algorithm that is implemented in UltraScan III (7). The calculations were performed on the UltraSan LIMS cluster at the Bioinformatics Core Facility at the University of Texas Health Science Center at San Antonio.

Table S1: Parameters obtained from the fluorescence quenching analysis using the Stern-Volmer plot.

Condition	**Stern-Volmer Constant (K_{SV}) (M^{-1})**
Native CcdB at pH 4	2.9 ± 0.4
Native CcdB at pH 7	2.9 ± 0.2
Unfolded CcdB at pH 4	12.1 ± 1.5

Table S2: Kinetic parameters for HX of CcdB at pH 4 and pH 7.

	Observed rate (s^{-1})		**Amplitude (Da)**	
	pH 4	pH 7	pH 4	pH 7
Fast phase	0.044 ±0.002	0.021 ± 0.002	12 ± 0.3	13 ± 1
Medium phase	0.003 ± 0.00008	0.0013 ± 0.0006	13 ± 0.3	10 ± 1
Slow phase	0.00007 ± 0.00002	0.0002 ± 0.00002	20 ± 0.003	15 ± 3

Table S3: Kinetic parameters for HX of peptides of CcdB at pH 4.

Peptide	Fast Phase		Medium Phase		Slow Phase	
	Amplitude (Da)	Observed Rate (s^{-1})	Amplitude (Da)	Observed Rate (s^{-1})	Amplitude (Da)	Observed Rate (s^{-1})
1-16	1.6	0.034	1.7	$3.4*10^{-3}$	1.8372	$7.5*10^{-5}$
17-23	0.5	0.021	0.6	$4.7*10^{-4}$	-	-
24-41	2.2	0.021	0.6	$9.3*10^{-4}$	-	-
42-60	3.6	0.015	1.8	$2.5*10^{-4}$	-	-
61-68	-	-	0.8	$2.3*10^{-3}$	1.3366	$6.4*10^{-5}$
80-96	-	-	3.2	$6.3*10^{-3}$	1.6110	$9.2*10^{-5}$

Table S4: Kinetic parameters for HX of peptides of CcdB at pH 7.

Peptide	Fast Phase		Medium Phase		Slow Phase	
	Amplitude (Da)	Observed Rate (s^{-1})	Amplitude (Da)	Observed Rate (s^{-1})	Amplitude (Da)	Observed Rate (s^{-1})
1-16	-	-	1.8652	$4.1*10^{-3}$	1.8094	$1.7*10^{-4}$
17-23	0.6214	0.0129	-	-	0.5893	$1.6*10^{-4}$
24-41	0.9119	0.2048	0.5549	$3.1*10^{-3}$	1.8655	$1.5*10^{-4}$
42-60	2.6012	0.0218	1.0889	$1.0*10^{-3}$	-	-
61-68	0.8195	0.0680	0.9498	$2.2*10^{-3}$	1.8308	$2.1*10^{-4}$
80-96	-	-	3.5053	$1.9*10^{-3}$	3.3792	$1.6*10^{-4}$

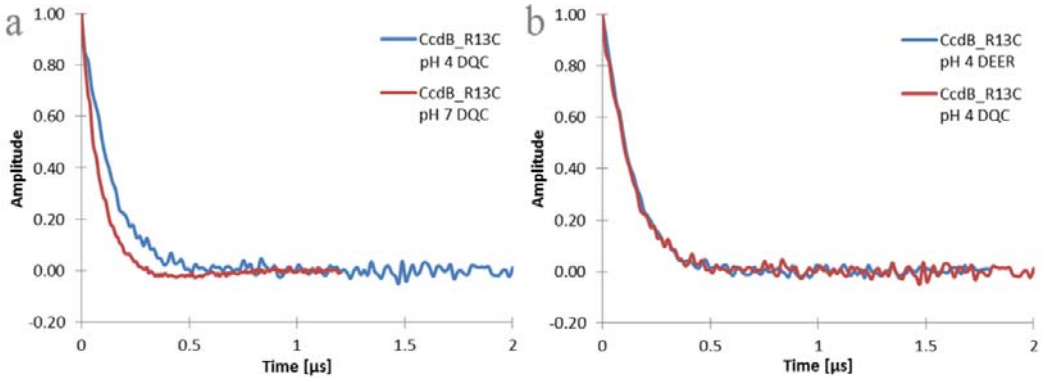

Figure S1: Normalized DQC and DEER EPR spectra in time-domain of the single cysteine variant of CcdB - R13C. (a) DQC spectra at pH 4.0 and pH 7.0. (b) DEER and DQC spectra at pH 4.0. The time-domain DEER data were in very good agreement with the respective DQC data, agreeing well, for example, in the bimodal characters and other details.

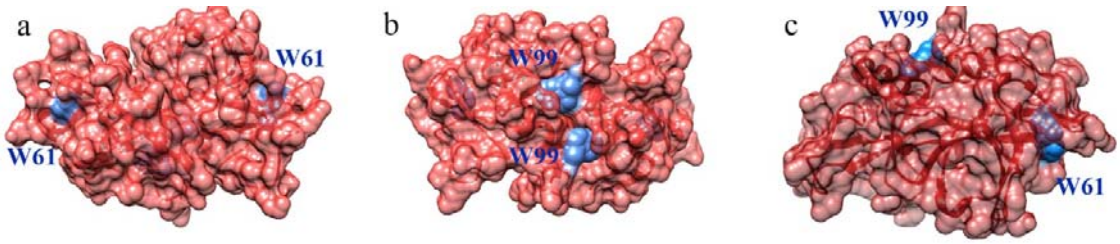

Figure S2: Solvent accessibility of the tryptophan residues in CcdB. Panel a, b and c show different views of the CcdB homodimer with tryptophan residues marked using blue color. Panel a shows the tryptophan residues located at position 61on both the monomers, where the Cα-Cα distance between them is 37 Å. Panel b shows tryptophan residues at position 99 located at the dimer interface on both the monomers having a Cα-Cα distance of 12 Å. Panel c shows the tryptophan residues 61 and 99 on a single monomer located at a Cα-Cα distance of 28 Å. All the tryptophan residues are significantly buried, which is consistent with the blue shifted fluorescence emission spectra (Figure 1c) of the native protein as compared to the unfolded protein (8).

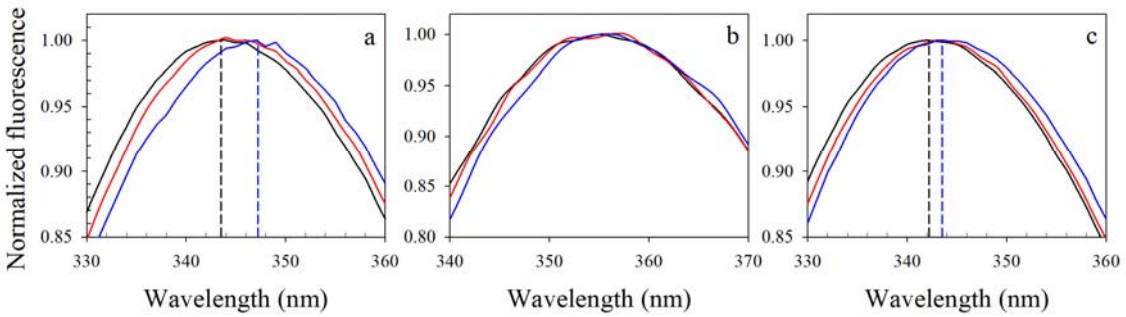

Figure S3: Dependence of the emission spectrum on the excitation wavelength. Panel a and b show the fluorescence emission spectra of native (20 mM sodium acetate buffer) and unfolded (3 M GdnHCl buffered using 20 mM sodium acetate) CcdB at pH 4, respectively, upon using excitation wavelengths of 295 nm (black line), 300 nm (red line) and 305 nm (blue line). Panel c shows fluorescence emission spectra of CcdB at pH 7 in native condition (10 mM HEPES buffer) obtained upon using excitation wavelength of 295 nm (black line), 300 nm (red line) and 305 nm (blue line). Black and blue dashed lines mark the maximum of the emission spectrum obtained using the excitation wavelengths of 295 nm and 305 nm, respectively. The fluorescence spectra were normalized to maximum intensity. The native form of CcdB shows a shift in emission wavelength with shift in excitation wavelength at both pH 4 and 7 with a larger shift at pH 4, whereas the unfolded protein does not show such dependence.

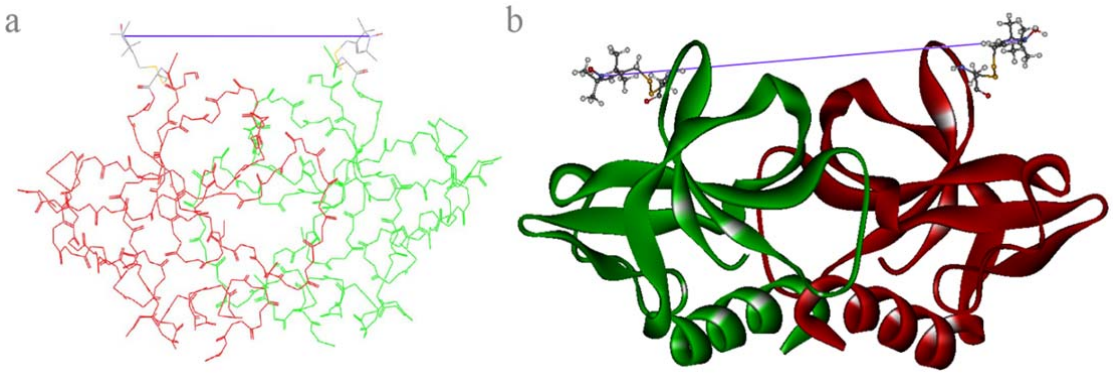

Figure S4: Simulated distance between the EPR spin labels for R13C variant of CcdB. Panel a and b shows the CcdB homodimer labeled with (1-oxyl-2,2,5,5-tetramethyl-pyrroline-3-methyl)-methanethiosulfonate (MTS). For the simulation the pdb entry 3VUB from the protein data bank RCSB PDB was used. In panel a, the traditional wire frame display is used to display atoms and non-bonded atoms are displayed as jacks. Panel b represents the protein backbone as a solid, 3D ribbon. EPR measurements were used to detect the distances between both nitroxides, as indicated in purple.

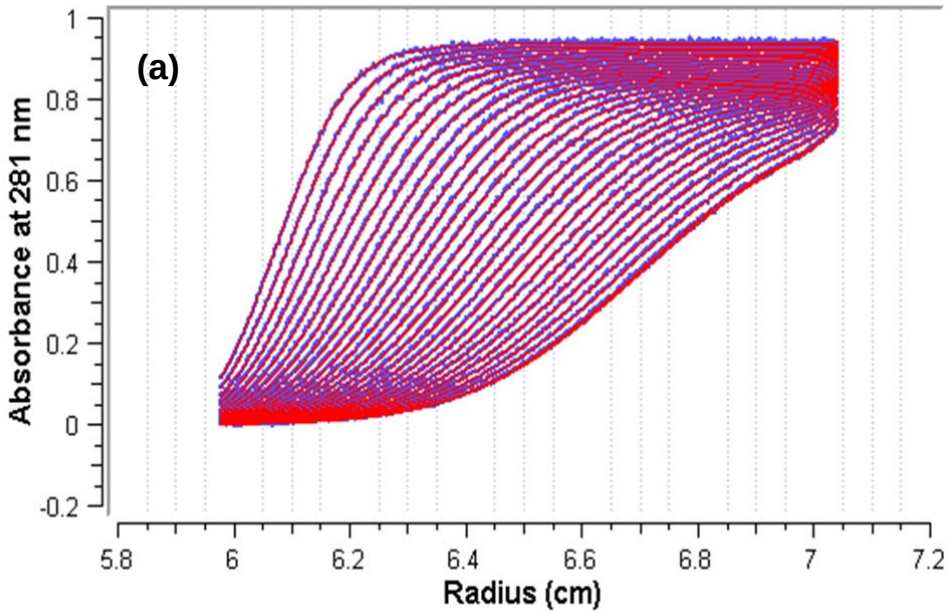
(a)
Absorbance at 281 nm
1
0.8
0.6
0.4
0.2
0
-0.2
5.8
6
6.2
6.4
6.6
6.8
7
7.2
Radius (cm)

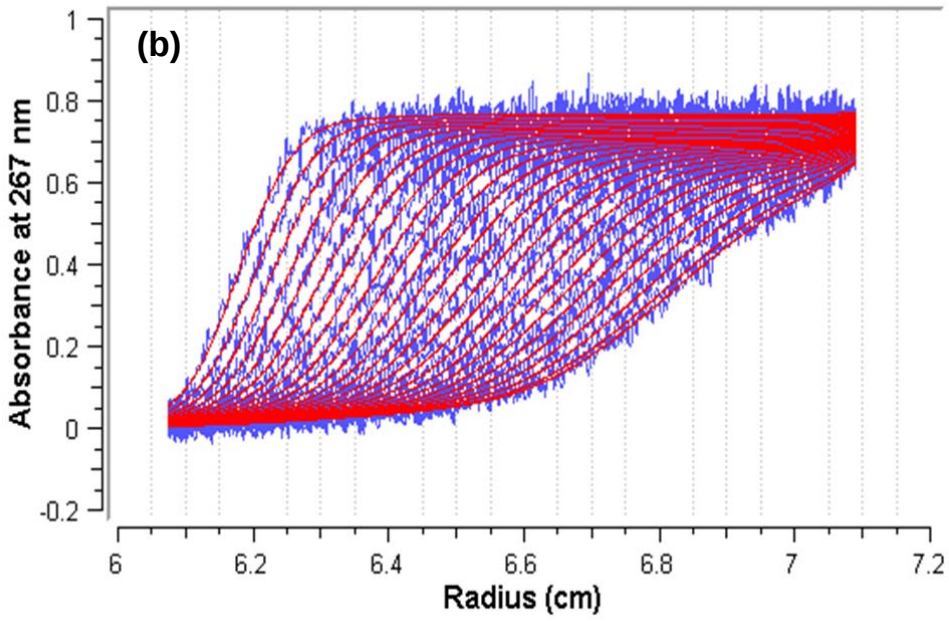
(b)
Absorbance at 267 nm
1
0.8
0.6
0.4
0.2
0
-0.2
6
6.2
6.4
6.6
6.8
7
7.2
Radius (cm)

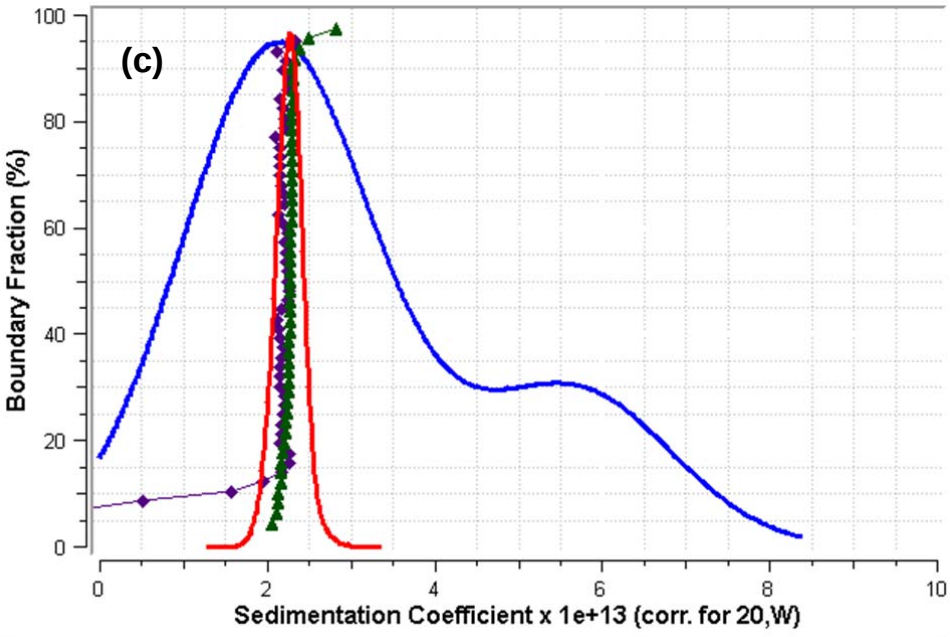
(c)
Boundary Fraction (%)
100
80
60
40
20
0
0
2
4
6
8
10
Sedimentation Coefficient x 1e+13 (corr. for 20,W)

Figure S5: Analytical ultracentrifugation studies confirm that CcdB at pH 4 is dimeric.

(a) and (b) show finite element fits of sedimentation velocity data of CcdB at pH 7 (10 mM Hepes, 50 mM NaCl) and at pH 4 (10mM Sodium acetate, 50 mM NaCl) respectively. The sedimentation was monitored by measuring absorbance at 281 nm and 267 nm, respectively across the length of the cell. Wavelength scans were taken at the start of the experiment to determine the λ_{max} for absorbance, for the given sample. The different traces represent overlays of absorbance measurements over time. The violet traces represent experimental data, while the red traces represent the fits. Only a few traces are shown for clarity. (c) The integral distribution plots (G(s)) and differential distribution plots (g(s)) obtained from the van Holde-Weischet analysis of the sedimentation velocity data for CcdB at pH 7 and at pH 4, have been overlaid. For CcdB at pH 7, the integral distribution is shown in green, while the differential distribution is shown as a red envelope. Similarly, for the pH 4 form, G(s) is shown is purple while g(s) is shown in blue. At pH's 7 and 4, about 90 % of the sample exists as a population with sedimentation coefficients of $2.2 \times 10^{-13} \pm 2.9 \times 10^{-15}$ s and $2.3 \times 10^{-13} \pm 1.3 \times 10^{-15}$ s respectively.

Plots (a), (b) and (c) were generated using the UltraScan III data analysis package (7).

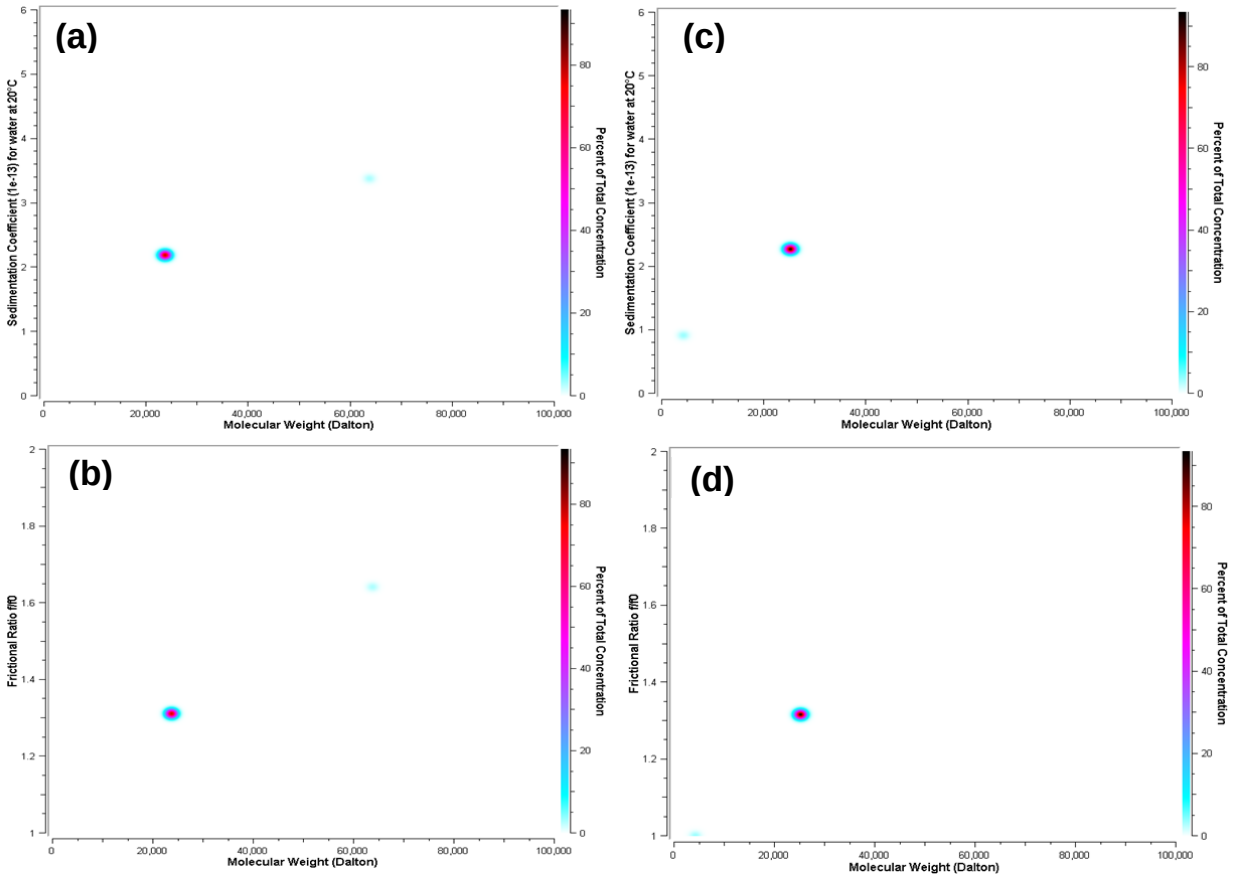

Figure S6: Analytical ultracentrifugation studies indicate that the mass of the low pH form of CcdB corresponds to that of the dimer.

Two-dimensional spectrum analysis (2-DSA)/Genetic algorithm analysis of sedimentation velocity data of CcdB at pH 7 (panels a and b) and at pH 4 (panels c and d). The color gradient indicates the fractional population of each species. Both the samples show the presence of a predominant dimeric form, with calculated molecular weight of ~25 kDa. Panels (a) and (c) show molecular weights of species with varied sedimentation coefficients. Panels (b) and (d) indicate that the frictional coefficient ratio (f/f0) for the predominant species at pH 7 and 4 are 1.3 under both conditions. A perfect sphere has a frictional ratio of 1. These plots were generated using the UltraScan III data analysis package (7).

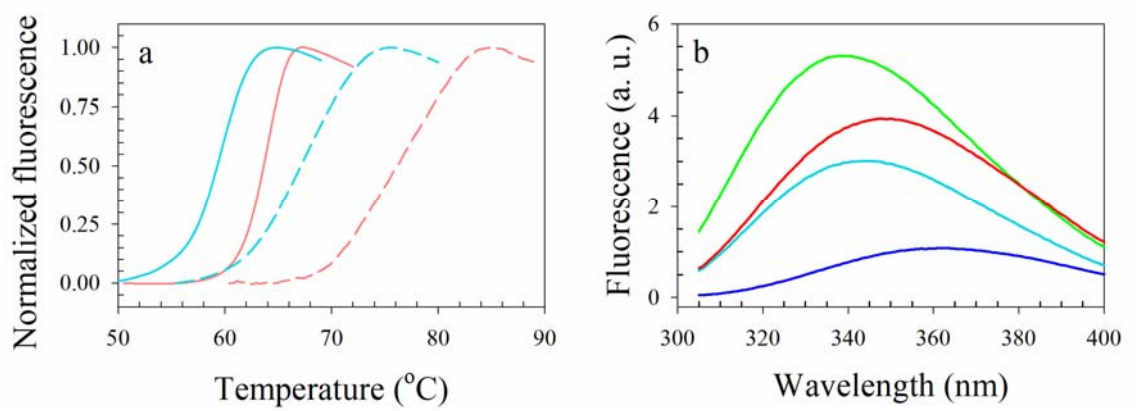

Figure S7: CcdA binding and thermal stability of CcdB. (a) Thermal unfolding profiles of 4μM CcdB at pH 7 (pink line) and pH 4 (cyan line) are shown. Unfolding was carried out in absence (solid lines) and in presence (dashed lines) of 10μM of $CcdA_{46\text{-}72}$ peptide. The change in fluorescence signal of SYPRO orange with respect to temperature was measured and a relative fluorescence plot was generated by normalizing the values in the transition region to the unfolded and folded baseline signals. Since this unfolding transition is not reversible, the midpoint of the thermal unfolding curve (the temperature at which 50% of the protein is unfolded) is taken to represent the apparent T_m of the protein. CcdB has lower thermal stability at pH 4 than at pH 7. Like the pH 7 form, the pH 4 form also binds the ligand CcdA, and the thermal stability is increased by ligand binding. (b) Intrinsic tryptophan fluorescence emission spectra acquired for CcdA (blue line), CcdB (cyan line) and CcdA-CcdB (green line) complex under native conditions at pH 4. The solid red line marks the arithmetic sum of fluorescence of CcdA and CcdB. The fluorescence spectrum of the CcdA-CcdB complex shows a blueshift as compared to the fluorescence spectrum of CcdA+CcdB (red line), confirming that CcdA binds to CcdB at pH 4.

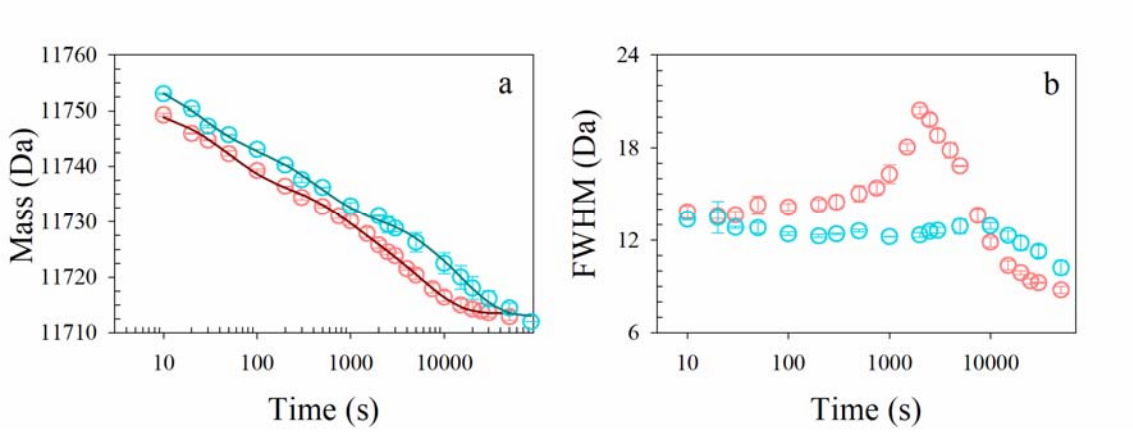

Figure S8: Effect of pH on hydrogen exchange rates of CcdB. Panel a shows mass of CcdB protein after various times of HX at pH 7 (red) and pH 4 (cyan) derived from the mass profiles shown in Figure 4. The solid lines through the data are fits to the data using a three-exponential equation. Panel b shows full width at half maxima (FWHM) obtained for each mass profile at pH 4 and pH 7. pH 7 data show a distinct increase in FWHM as compared to that of pH 4 data, suggesting EXX exchange. Error bars represent standard errors from two independent experiments.

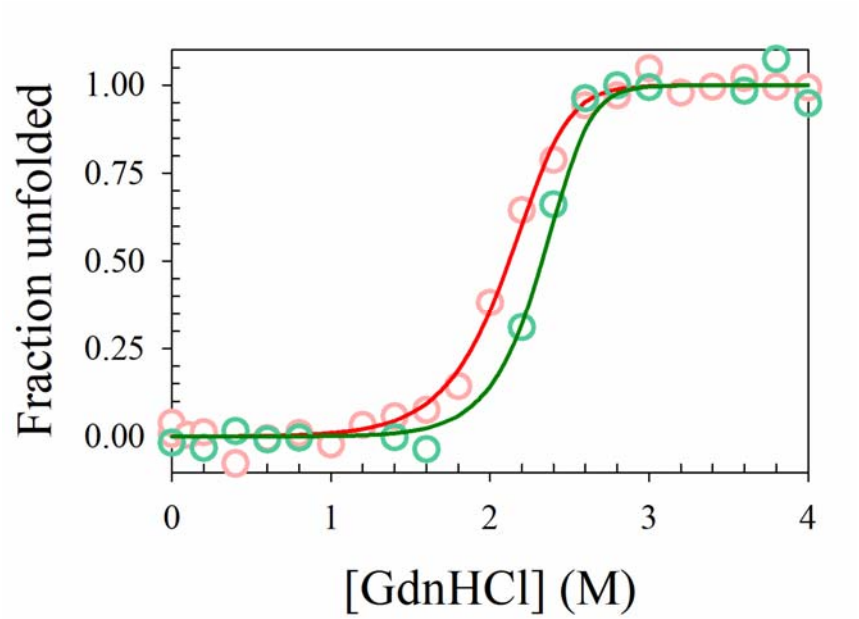

Figure S9: Effect of pH on the stability of CcdB. GdnHCl induced equilibrium unfolding transitions of CcdB at pH 4 (red) and pH 7 (green) obtained at 4 μM monomeric protein concentration. The equilibrium unfolding transitions were obtained by monitoring intrinsic tryptophan fluorescence at 385 nm upon exciting at 280 nm. The solid lines through the data are fits obtained using a two-state homodimeric unfolding model (9). The obtained values of ΔG^{o}_{U} of CcdB at pH 4 and 7 were 16.1 kcal mol^{-1} and 19.9 kcal mol^{-1}, respectively.

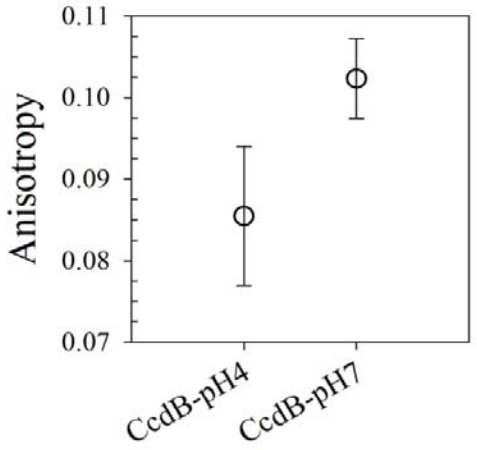

Figure S10: Anisotropy measurements of tryptophan residues at pH 4 and pH 7. Steady state anisotropy of CcdB was measured at pH 4 and pH 7 to probe the change in compaction of the protein core. Expansion of the core of the protein will likely result in decrease in the value of the anisotropy of the tryptophan due to an increase in the freedom of rotation of the tryptophan residues. Marginal but consistent change in anisotropy was observed, which suggests expansion of the core of the protein.

Supporting References:

1. Niesen, F. H., H. Berglund, and M. Vedadi. 2007. The use of differential scanning fluorimetry to detect ligand interactions that promote protein stability. Nat Protoc 2(9):2212-2221.

2. Demeler, B. 2005. UltraScan - A Comprehensive Data Analysis Software Package for Analytical Ultracentrifugation Experiments. Analytical Ultracentrifugation: Techniques and Methods. D. J. Scott, S. E. Harding, and A. J. Rowe, editors. The Royal Society of Chemistry, pp. 210-230.

3. Laue, T., D. Shah, T. Ridgeway, and S. Pelletier. 1992. Computer-aided interpretation of analytical sedimentation data for proteins. Cambridge: Society of Chemistry. .

4. Brookes, E., W. Cao, and B. Demeler. 2010. A two-dimensional spectrum analysis for sedimentation velocity experiments of mixtures with heterogeneity in molecular weight and shape. Eur Biophys J 39(3):405-414.

5. Demeler, B., and E. Brookes. 2008. Monte Carlo analysis of sedimentation experiments. Colloid and Polymer Science 286(2):129-137. journal article.

6. Brookes, E., and B. Demeler. 2006. Genetic Algorithm Optimization for Obtaining Accurate Molecular Weight Distributions from Sedimentation Velocity Experiments. Analytical Ultracentrifugation VIII. C. Wandrey and H. Cölfen, editors. Springer Berlin Heidelberg, Berlin, Heidelberg, pp. 33-40.

7. Demeler, B., H. Saber, and J. C. Hansen. 1997. Identification and interpretation of complexity in sedimentation velocity boundaries. Biophys J 72(1):397-407.

8. Baliga, C., R. Varadarajan, and N. Aghera. 2016. Homodimeric Escherichia coli Toxin CcdB (Controller of Cell Division or Death B Protein) Folds via Parallel Pathways. Biochemistry 55(43):6019-6031.

9. Bajaj, K., G. Chakshusmathi, K. Bachhawat-Sikder, A. Surolia, and R. Varadarajan. 2004. Thermodynamic characterization of monomeric and dimeric forms of CcdB (controller of cell division or death B protein). Biochem J 380(Pt 2):409-417.